Matthias Glätzle and Hubert Huppertz*

$RE_4B_4O_{11}F_2$ (*RE* = Sm, Tb, Ho, Er): four new rare earth fluoride borates isotypic to $Gd_4B_4O_{11}F_2$

DOI 10.1515/znb-2016-0123
Received May 5, 2016; accepted May 20, 2016

Abstract: The rare earth fluoride borates $RE_4B_4O_{11}F_2$ (*RE* = Sm, Tb, Ho, Er) were synthesized in a Walker-type multi-anvil apparatus from the corresponding rare earth oxides and fluorides with boron oxide. $Sm_4B_4O_{11}F_2$ was obtained under high-pressure/high-temperature conditions of 6 GPa/1100°C, $Tb_4B_4O_{11}F_2$ at 7.5 GPa/1200°C, and $Ho_4B_4O_{11}F_2$ and $Er_4B_4O_{11}F_2$ at 9.5 GPa/1300°C. The single-crystal structure determinations showed that all compounds are isotypic to the known rare earth fluoride borates $RE_4B_4O_{11}F_2$ (*RE* = Pr, Nd, Eu, Gd, Dy). They crystallize in the monoclinic space group *C*2/*c* (*Z* = 4). The structure is built up from BO_4 tetrahedra as well as BO_3 groups connected *via* common corners. Here, we report about the crystallographic characterization of these new compounds in comparison to the isotypic phases $RE_4B_4O_{11}F_2$ (*RE* = Pr, Nd, Eu, Gd, Dy).

Keywords: borate; crystal structure; fluoride; high pressure; rare earth.

1 Introduction

Borates are well known for their extraordinary optical properties with a very high transparency into the deep UV. Therefore, they may be used as host materials for luminescent and nonlinear-optical applications. Some fluoride borates exhibit an even larger optical gap due to the incorporation of fluorine atoms [1, 2]. Rare earth fluoride borates also show very interesting luminescence, fluorescence, and dielectric properties [3–6]. These compounds can be prepared with remarkable complexity. Borates in general form some of the most diverse structures because both planar BO_3 as well as tetrahedral BO_4 groups can be present and interconnected *via* common corners and/or edges. Recently, the structural motive of linear BO_2 groups was confirmed by Höppe in the gadolinium borate fluoride oxide $Gd_4(BO_2)O_5F$ [7]. In combination with the wide range of possible coordination numbers of lanthanides, these compounds are very interesting for ongoing investigations.

For the synthesis of new rare earth fluoride borates, we apply high-pressure/high-temperature conditions. This has led to the finding of more than 20 new rare earth fluoride borates crystallizing in various structure types. A summary of the achievements reached so far can be found in Refs. [8, 9].

For the chemical composition $RE_4B_4O_{11}F_2$, two different structure types were obtained by high-pressure/high-temperature syntheses. In 2010, Haberer et al. presented the compound $La_4B_4O_{11}F_2$ [10] crystallizing in space group $P2_1/c$ with the lattice parameters a = 778.1(2), b = 3573.3(7), c = 765.7(2) pm, and β = 113.92(3)° (Z = 8). The crystal structure consists of BO_3 groups (Δ) which are either isolated (Δ), connected *via* common corners (ΔΔ), or connected *via* BO_4 tetrahedra forming the fundamental building block (FBB) 2Δ□:Δ□Δ (after Burns et al. [11]).

Earlier in 2010, Haberer et al. discovered the fluoride borate $Gd_4B_4O_{11}F_2$ [12] showing the same atomic composition $RE_4B_4O_{11}F_2$ but a completely different crystal structure in space group *C*2/*c*. The crystal structure of $Gd_4B_4O_{11}F_2$ contains BO_3 groups and BO_4 tetrahedra connected *via* common corners. The structural motif consists of two BO_3 groups (Δ) and two BO_4 tetrahedra (□), and can be described with the fundamental building block 2Δ2□:Δ□□Δ, which represented a novelty in borate chemistry. Later in 2010, Haberer et al. were able to synthesize two compounds crystallizing isotypically to $Gd_4B_4O_{11}F_2$, namely $Eu_4B_4O_{11}F_2$ and $Dy_4B_4O_{11}F_2$ [13]. With the syntheses of $Pr_4B_4O_{11}F_2$ and $Nd_4B_4O_{11}F_2$ [14], we succeeded in the synthesis of two more isotypic compounds in 2013. To discover possibly all compounds $RE_4B_4O_{11}F_2$ that are isotypic to $Gd_4B_4O_{11}F_2$, we continued our investigations in synthesizing all other rare earth fluoride borates with this composition not described in literature so far. Finally, we succeeded in the synthesis of $RE_4B_4O_{11}F_2$ with *RE* = Sm, Tb, Ho, Er.

***Corresponding author: Hubert Huppertz,** Institut für Allgemeine, Anorganische und Theoretische Chemie, Leopold-Franzens-Universität Innsbruck, Innrain 80–82, A-6020 Innsbruck, Austria, Fax: +43 512 507 57099,
E-mail: Hubert.Huppertz@uibk.ac.at
Matthias Glätzle: Institut für Allgemeine, Anorganische und Theoretische Chemie, Leopold-Franzens-Universität Innsbruck, Innrain 80–82, A-6020 Innsbruck, Austria

In the following, we report about the four newly synthesized compounds $RE_4B_4O_{11}F_2$ (RE = Sm, Tb, Ho, Er), which are all isotypic to $RE_4B_4O_{11}F_2$ (RE = Pr, Nd, Eu, Gd, Dy) [12, 13]. The syntheses and structural properties of $RE_4B_4O_{11}F_2$ (RE = Sm, Tb, Ho, Er) are discussed in comparison to the isotypic compounds.

2 Experimental part

2.1 Syntheses

All new compounds $RE_4B_4O_{11}F_2$ (RE = Sm, Tb, Ho, Er) were synthesized under high-pressure/high-temperature conditions in a Walker-type multianvil apparatus. Reactions of the oxides Sm_2O_3, Tb_4O_7, Ho_2O_3, and Er_2O_3 with the corresponding rare earth fluorides REF_3 (RE = Sm, Tb, Ho, Er) and B_2O_3 led to the formation of the products according to the following Eqs. 1–4.

$$5\,Sm_2O_3 + 2\,SmF_3 + 6\,B_2O_3 \xrightarrow[1100°C]{6\,GPa} 3\,Sm_4B_4O_{11}F_2 \quad (1)$$

$$5\,Tb_4O_7 + 4\,TbF_3 + 12\,B_2O_3 \xrightarrow[1200°C]{7.5\,GPa} 6\,Tb_4B_4O_{11}F_2 + 5/2\,O_2 \quad (2)$$

$$5\,Ho_2O_3 + 2\,HoF_3 + 6\,B_2O_3 \xrightarrow[1300°C]{9.5\,GPa} 3\,Ho_4B_4O_{11}F_2 \quad (3)$$

$$5\,Er_2O_3 + 2\,ErF_3 + 6\,B_2O_3 \xrightarrow[1300°C]{9.5\,GPa} 3\,Er_4B_4O_{11}F_2 \quad (4)$$

Stoichiometric mixtures of Sm_2O_3 (Strem Chemicals, Newburyport, MA, USA, 99.9%), Tb_4O_7 (Smart Elements, Vienna, Austria, 99.99%), Ho_2O_3 (Strem Chemicals, Newburyport, MA, USA, 99.9%), or Er_2O_3 (Strem Chemicals, Newburyport, MA, USA, 99.9%) with the corresponding rare earth fluoride SmF_3, TbF_3, HoF_3, or ErF_3 (each from Strem Chemicals, Newburyport, MA, USA, 99.9%) and B_2O_3 (Strem Chemicals, Newburyport, MA, USA, 99.9+%) were finely ground inside a glove box under argon inert gas atmosphere and filled into boron nitride crucibles (Henze Boron Nitride Products GmbH, HeBoSint® P100, Kempten, Germany). These crucibles were placed into the center of 14/8 or 18/11 assemblies and compressed by eight tungsten carbide cubes (Hawedia, ha-7%Co, Marklkofen, Germany). Pressure was applied *via* a 1000 ton press with a modified multianvil Walker module (both devices from the company Voggenreiter, Mainleus, Germany). A detailed description of the construction of the assembly is given in Refs. [15–19].

For the synthesis of $Sm_4B_4O_{11}F_2$, the educt mixture inside the 18/11 assembly was compressed up to 6 GPa in 150 min, keeping it at this pressure for the following heating period. The temperature was then increased to 1100°C in 10 min, kept there for 15 min, and decreased to 500°C in 35 min and finally to room temperature by switching off the heating. This program was followed by a decompression period of 7.5 h. $Tb_4B_4O_{11}F_2$ was synthesized by compressing the 14/8 assembly up to 7.5 GPa within 160 min, heating it up to 1200°C in the following 10 min, holding the temperature for another 15 min and cooling it down to 500°C within 20 min. After natural cooling down to room temperature by switching off the heating, the sample was decompressed in about 8 h. For the syntheses of $Ho_4B_4O_{11}F_2$ and $Er_4B_4O_{11}F_2$, the educt mixtures in the 14/8 assemblies were compressed to 9.5 GPa in 210 min. Afterwards, the samples were heated up to 1300°C within 10 min, kept there for 8 min and cooled down to 650°C in 25 min at constant pressure. The temperature was decreased to room temperature by switching off the heating, and the samples were decompressed within 11 h.

The recovered MgO octahedra (Ceramic Substrates & Components Ltd., Newport, Isle of Wight, UK) were broken apart and the samples carefully separated from the surrounding boron nitride crucibles. While $Sm_4B_4O_{11}F_2$ and $Tb_4B_4O_{11}F_2$ were obtained as colorless, air- and water-resistant crystals, and $Er_4B_4O_{11}F_2$ as pink crystals, $Ho_4B_4O_{11}F_2$ showed a very intense alexandrite effect (daylight: yellow, incandescent light: pink).

2.2 Crystal structure analyses

The isotypic compounds $RE_4B_4O_{11}F_2$ (RE = Sm, Tb, Ho, Er) were characterized by powder X-ray diffraction. The powder diffraction patterns were obtained in transmission geometry from a flat sample of the reaction products, using a Stoe Stadi P powder diffractometer with $MoK_{\alpha 1}$ radiation [Ge(111)-monochromatized, λ = 70.93 pm]. The powder diffraction patterns showed the reflections of the new rare earth fluoride borates as the main products in all cases. While the powder patterns of the samples of $Tb_4B_4O_{11}F_2$ and $Ho_4B_4O_{11}F_2$ contained only very weak reflections caused by a still unknown phase, the side products of the syntheses of $Sm_4B_4O_{11}F_2$ and $Er_4B_4O_{11}F_2$ could be identified by reflection patterns of α-$Sm_2B_4O_9$ [20] and $Er_3B_5O_{12}$ [21], respectively. Figure 1 shows the powder pattern of $Ho_4B_4O_{11}F_2$ with some weak reflections of the unknown side product (marked with asterisks). The experimental powder pattern (top) is in good agreement with the theoretical pattern (bottom), simulated from the single-crystal data. By indexing the reflections of the samarium fluoride borate, the parameters a = 1373.83(7), b = 466.53(3), c = 1380.82(8)

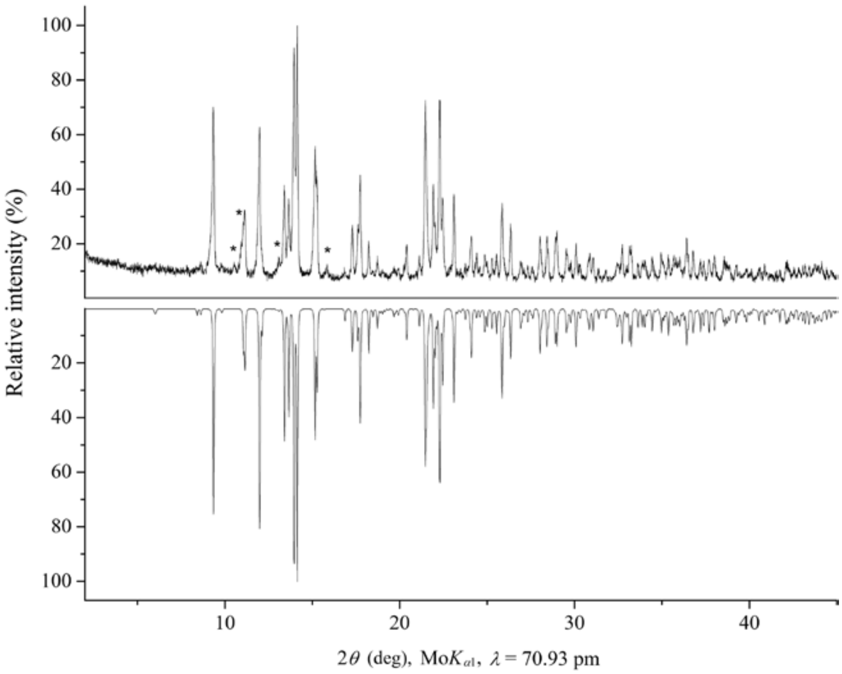

Fig. 1: Top: experimental powder X-ray diffraction pattern of $Ho_4B_4O_{11}F_2$; the reflections of an unknown side product are indicated with asterisks. Bottom: theoretical powder pattern of $Ho_4B_4O_{11}F_2$, based on single-crystal diffraction data.

pm, β = 91.09(1)°, and a volume of 0.88486(6) nm^3 were obtained. The indexing of the corresponding terbium fluoride borate powder diffraction pattern led to the parameters a = 1355.35(7), b = 461.99(3), c = 1367.17(9) pm, β = 91.20(1)°, and a volume of 0.85588(6) nm^3. For $Ho_4B_4O_{11}F_2$, the indexing of the powder diffraction pattern resulted in the parameters a = 1342.93(6), b = 459.84(3), c = 1359.08(7) pm, β = 91.38(1)°, and a volume of 0.83903(5) nm^3, and for $Er_4B_4O_{11}F_2$, the parameters a = 1337.4(9), b = 458.9(3), c = 1352.9(8) pm, β = 91.4(1)°, and a volume of 0.8301(7) nm^3 were obtained. These data validated the lattice parameters obtained from the single-crystal X-ray diffraction data for $RE_4B_4O_{11}F_2$ (RE = Sm, Tb, Ho, Er) (Table 1).

For the single-crystal structure analyses, small single crystals of all four new compounds were isolated by mechanical fragmentation. The intensity data of the single-crystals were collected at room temperature with a Kappa CCD diffractometer (Bruker AXS/Nonius, Karlsruhe, Germany) equipped with a Miracol fiber optics collimator and a Nonius FR590 generator (graphite-monochromatized MoK_α radiation, λ = 71.073 pm). Semiempirical absorption corrections based on equivalent and redundant intensities were applied with the program Scalepack [22]. According to the systematic extinctions, the monoclinic spacegroup $C2/c$ was derived for the four isotypic compounds. Because of the fact that all four new compounds crystallize isotypic to $Gd_4B_4O_{11}F_2$, the positional parameters of $Gd_4B_4O_{11}F_2$ were used as starting values for the structural refinement [12]. The parameter refinements (full-matrix least-squares on F^2) were achieved by using the Shelxs/l-97 software suite [23, 24]. All atoms could be refined with anisotropic displacement parameters. Final difference Fourier syntheses did not reveal any significant peaks in the refinements. All relevant details of the data collections and evaluations are given in Table 1. The positional parameters, interatomic distances, and interatomic angles are listed in the Tables 2–4.

Additional details of the crystal structure investigations may be obtained from the Fachinformationszentrum Karlsruhe, 76344 Eggenstein-Leopoldshafen, Germany (fax: +49-7247-808-666; e-mail: crysdata@fiz-karlsruhe.de, https://icsd.fiz-karlsruhe.de/search/basic.xhtml) on quoting the deposition numbers CSD-427586 for $Sm_4B_4O_{11}F_2$, CSD-427587 for $Tb_4B_4O_{11}F_2$, CSD-427588 for $Ho_4B_4O_{11}F_2$, and CSD-427589 for $Er_4B_4O_{11}F_2$.

3 Results and discussion

As reported for the previously published isotypic phases $RE_4B_4O_{11}F_2$ (RE = Pr, Nd, Eu, Gd, Dy) [12–14], these compounds are formed in a wide pressure and temperature range. Therefore, we were interested to investigate the possibility to synthesize more compounds with the same composition and crystal structure using different rare earth

Table 1: Crystal data and numbers pertinent to data collection and structure refinement of $RE_4B_4O_{11}F_2$ (RE = Sm, Tb, Ho, Er) (standard deviations in parentheses).

Empirical formula	$Sm_4B_4O_{11}F_2$	$Tb_4B_4O_{11}F_2$	$Ho_4B_4O_{11}F_2$	$Er_4B_4O_{11}F_2$
M_r	858.64	892.92	916.96	926.28
Crystal system		Monoclinic		
Space group		$C2/c$		
Powder diffractometer		Stoe Stadi P		
Radiation; λ, pm		Mo$K_{\alpha1}$; 70.93 (Ge(111) monochromator)		
Powder data				
a, pm	1373.83(7)	1355.35(7)	1342.93(6)	1337.4(9)
b, pm	466.53(3)	461.99(3)	459.84(3)	458.9(3)
c, pm	1380.82(8)	1367.17(9)	1359.08(7)	1352.9(8)
β, deg	91.09(1)	91.20(1)	91.38(1)	91.4(1)
V, nm^3	0.88486(6)	0.85588(6)	0.83903(5)	0.8301(7)
Single-crystal diffractometer		Nonius Kappa CCD		
Radiation; λ, pm		MoK_{α}; 71.073 (graphite monochromator)		
Single-crystal data				
a, pm	1375.06(1)	1356.0(3)	1343.3(3)	1337.0(3)
b, pm	466.95(2)	462.20(9)	459.99(9)	458.82(9)
c, pm	1381.66(4)	1368.1(3)	1359.2(3)	1355.4(3)
β, deg	91.1(1)	91.2(1)	91.4(1)	91.4(1)
V, nm^3	0.88698(5)	0.8573(3)	0.8396(3)	0.8312(3)
Formula units per cell		$Z = 4$		
Calculated density, g cm^{-3}	6.43	6.92	7.25	7.40
Crystal size, mm^3	0.04 × 0.03 × 0.01	0.03 × 0.03 × 0.02	0.03 × 0.02 × 0.01	0.03 × 0.02 × 0.01
Temperature, K	293(2)	293(2)	293(2)	293(2)
Absorption coefficient, mm^{-1}	26.2	32.7	37.4	40.1
F(000), e	1496	1544	1576	1592
θ range, deg	1.00 37.79	1.00 37.79	1.00 37.79	1.00 37.79
Range in hkl	±20, ±7, ±20	−20:19, ±6, ±20	±22, ±7, −21:23	±22, ±7, ±23
Total no. of reflections	17093	13407	15732	13199
Independent reflections/R_{int}	5884/0.0690	4893/0.0570	7576/0.0613	8003/0.0643
Reflections with $I > 2\sigma(I)/R_\sigma$	1476/0.0448	1266/0.0445	1853/0.0452	1723/0.0461
Data/ref. parameters	1594/97	1546/97	2235/97	2220/97
Absorption correction		Multi-scan (SCALEPACK [22])		
Goodness-of-fit on F^2	1.098	1.077	1.067	1.037
Final indices R_1/wR_2 [$I > 2\sigma(I)$]	0.0240/0.0638	0.0288/0.0657	0.0304/0.0765	0.0299/0.0693
Indices R_1/wR_2 (all data)	0.0259/0.0650	0.0392/0.0696	0.0381/0.0808	0.0425/0.0767
Largest diff. peak/hole, × 10^{-6} e pm^{-3}	2.94/−2.24	3.07/−2.25	2.70/−3.53	3.60/−3.98

metal cations. While various syntheses applying different pressure and temperature conditions yielded the desired new phases $RE_4B_4O_{11}F_2$ (RE = Sm, Tb) as the main products, the syntheses of $Ho_4B_4O_{11}F_2$ and $Er_4B_4O_{11}F_2$ were only successful in a small pressure and temperature range, namely 9–10 GPa at about 1300°C. At lower pressure conditions, the main products of the syntheses were the rare earth oxides and rare earth fluoride oxides. Higher pressure conditions resulted in the formation of a new and not yet completely characterized product. While $Tb_4B_4O_{11}F_2$ and $Ho_4B_4O_{11}F_2$ could be obtained as phase pure products, the synthesis of $Sm_4B_4O_{11}F_2$ led to the formation of small amounts of α-$Sm_2B_4O_9$ [20] as a byproduct. The reaction products of the syntheses of $Er_4B_4O_{11}F_2$ also contained significant amounts of $Er_3B_5O_{12}$ [21] and a yet unknown byproduct.

As reported last year [14], the synthesis of "$Ce_4B_4O_{11}F_2$" has been attempted several times in our group using various reaction conditions, but without any success. Likewise, the synthesis of the compounds "$RE_4B_4O_{11}F_2$ (RE = Tm, Yb, Lu)" could not be achieved up to now. Interestingly, $La_4B_4O_{11}F_2$ [10] is still the only known rare earth fluoride borate with the same composition but a completely different crystal structure.

The structure of $RE_4B_4O_{11}F_2$ (RE = Sm, Tb, Ho, Er) contains planar BO_3 groups as well as BO_4 tetrahedra connected *via* common corners, as it is shown in Fig. 2. Two BO_3 groups (Δ) and two BO_4 tetrahedra (□) build up the main structural motif. This has first been discovered in $Gd_4B_4O_{11}F_2$ and can be described with the fundamental building block 2Δ2□:Δ□□Δ. A detailed depiction of the

Table 2: Atomic coordinates and isotropic equivalent displacement parameters (U_{eq} in Å²) for $RE_4B_4O_{11}F_2$ (RE = Sm, Tb, Ho, Er) (space group: $C2/c$) standard deviations in parentheses. U_{eq} is defined as one third of the trace of the orthogonalized U_{ij} tensor.

Atom	Wyckoff position	x	y	z	U_{eq}
Sm1	8f	0.058848(16)	0.52088(4)	0.370591(13)	0.00573(9)
Sm2	8f	0.279341(15)	0.01801(4)	0.370945(14)	0.00559(9)
B1	8f	0.9071(3)	0.9789(8)	0.2856(3)	0.0056(7)
B2	8f	0.0948(3)	0.9543(9)	0.5254(3)	0.0070(7)
F1	8f	0.2306(2)	0.5243(5)	0.4252(2)	0.0126(5)
O1	8f	0.91191(18)	0.8687(6)	0.39347(17)	0.0070(4)
O2	8f	0.17286(19)	0.8147(5)	0.25790(17)	0.0075(4)
O3	8f	0.07902(18)	0.6653(6)	0.53520(17)	0.0075(4)
O4	4e	0	0.8487(8)	¼	0.0061(6)
O5	8f	0.1140(2)	0.0592(6)	0.43552(19)	0.0091(5)
O6	8f	0.90074(19)	0.2799(6)	0.27480(17)	0.0082(5)
Tb1	8f	0.05869(2)	0.51813(6)	0.370427(19)	0.00679(10)
Tb2	8f	0.279965(19)	0.01583(6)	0.370537(19)	0.00617(10)
B1	8f	0.9073(5)	0.9764(13)	0.2862(5)	0.0082(11)
B2	8f	0.0954(5)	0.9561(14)	0.5238(5)	0.0083(11)
F1	8f	0.2311(3)	0.5271(7)	0.4241(3)	0.0144(7)
O1	8f	0.9132(3)	0.8646(8)	0.3947(3)	0.0061(7)
O2	8f	0.1749(3)	0.8139(8)	0.2569(3)	0.0071(7)
O3	8f	0.0786(3)	0.6669(8)	0.5339(3)	0.0072(7)
O4	4e	0	0.8436(11)	¼	0.0059(10)
O5	8f	0.1154(3)	0.0645(9)	0.4331(3)	0.0103(8)
O6	8f	0.9014(3)	0.2800(8)	0.2760(3)	0.0069(7)
Ho1	8f	0.05840(2)	0.51584(4)	0.37029(2)	0.00782(7)
Ho2	8f	0.28056(2)	0.01404(4)	0.37002(2)	0.00723(7)
B1	8f	0.9066(4)	0.9744(9)	0.2867(4)	0.0092(8)
B2	8f	0.0964(4)	0.9602(10)	0.5227(4)	0.0087(7)
F1	8f	0.2316(2)	0.5281(6)	0.4237(3)	0.0155(6)
O1	8f	0.9126(2)	0.8591(6)	0.3954(2)	0.0071(5)
O2	8f	0.1768(2)	0.8137(7)	0.2569(2)	0.0097(5)
O3	8f	0.0791(2)	0.6670(6)	0.5330(2)	0.0094(5)
O4	4e	0	0.8381(9)	¼	0.0064(6)
O5	8f	0.1163(2)	0.0659(7)	0.4312(2)	0.0107(5)
O6	8f	0.9026(2)	0.2811(6)	0.2768(2)	0.0094(5)
Er1	8f	0.05858(2)	0.51476(4)	0.37005(2)	0.00688(7)
Er2	8f	0.28092(2)	0.01168(4)	0.36986(2)	0.00611(7)
B1	8f	0.9066(4)	0.972(1)	0.2864(4)	0.0077(8)
B2	8f	0.0966(4)	0.962(2)	0.5212(5)	0.0101(9)
F1	8f	0.2314(3)	0.5297(6)	0.4244(3)	0.0144(6)
O1	8f	0.9124(2)	0.8566(7)	0.3960(2)	0.0065(5)
O2	8f	0.1773(2)	0.8114(7)	0.2565(3)	0.0081(6)
O3	8f	0.0779(3)	0.6661(7)	0.5319(3)	0.0085(6)
O4	4e	0	0.8355(9)	¼	0.0071(8)
O5	8f	0.1165(3)	0.0677(7)	0.4299(3)	0.0086(6)
O6	8f	0.9027(3)	0.2801(7)	0.2773(3)	0.0082(6)

crystal structure of $RE_4B_4O_{11}F_2$ (RE = Sm, Tb, Ho, Er) can be found in the description of the isotypic compound $Gd_4B_4O_{11}F_2$ [12]. This paper gives a comparison and overview of the structural properties of all nine isotypic compounds $RE_4B_4O_{11}F_2$ (RE = Pr, Nd, Sm–Er).

Figure 3 shows a comparison of the lattice parameters of $Pr_4B_4O_{11}F_2$ [14], $Nd_4B_4O_{11}F_2$ [14], $Sm_4B_4O_{11}F_2$, $Eu_4B_4O_{11}F_2$ [13], $Gd_4B_4O_{11}F_2$ [12], $Tb_4B_4O_{11}F_2$, $Dy_4B_4O_{11}F_2$ [13], $Ho_4B_4O_{11}F_2$, and $Er_4B_4O_{11}F_2$. The exact values are given in Table 5. The difference of the lattice parameters corresponds to the decreasing ionic radii of the rare earth cations, well known as the lanthanide contraction. The values for the ionic radii of ninefold coordinated lanthanide cations as given in literature [25] are as follows: Pr^{3+} (131.9 pm), Nd^{3+} (130.3 pm),

Table 3: Interatomic distances (pm) in $RE_4B_4O_{11}F_2$ (RE = Sm, Tb, Ho, Er) (space group: $C2/c$), calculated with the single-crystal lattice parameters (standard deviations in parentheses).

Sm1–O6a	237.8(2)	Sm2–O2a	232.3(3)	B1–O6	141.6(4)
Sm1–O3a	238.3(2)	Sm2–O2b	235.9(2)	B1–O2	146.0(5)
Sm1–O4	239.2(2)	Sm2–O6	242.3(2)	B1–O4	150.6(5)
Sm1–O5a	245.0(3)	Sm2–O1	246.6(3)	B1–O1	157.6(5)
Sm1–F1	246.5(3)	Sm2–O5	246.5(3)		ø = 149.0
Sm1–O3b	247.8(2)	Sm2–O3	247.2(2)		
Sm1–O1	261.6(3)	Sm2–F1a	251.9(2)	B2–O5	136.5(5)
Sm1–O2	261.9(3)	Sm2–F1b	257.3(2)	B2–O3	137.4(5)
Sm1–O6b	276.3(3)	Sm2–F1c	282.9(3)	B2–O1	139.8(5)
Sm1–O5b	277.0(3)		ø = 249.2		ø = 137.9
	ø = 253.1				
Tb1–O3a	234.9(4)	Tb2–O2a	228.5(4)	B1–O6	141.2(7)
Tb1–O4	235.7(3)	Tb2–O2b	231.5(4)	B1–O2	145.8(8)
Tb1–O6a	235.9(4)	Tb2–O6	238.0(4)	B1–O4	149.3(7)
Tb1–O5a	238.6(4)	Tb2–O5	241.7(4)	B1–O1	157.2(8)
Tb1–F1	243.6(4)	Tb2–O1	243.9(4)		ø = 148.4
Tb1–O3b	245.3(4)	Tb2–O3	244.8(4)		
Tb1–O1	256.8(4)	Tb2–F1a	247.0(3)	B2–O3	136.3(7)
Tb1–O2	262.1(4)	Tb2–F1b	256.5(3)	B2–O5	137.1(8)
Tb1–O6b	270.5(4)	Tb2–F1c	282.4(4)	B2–O1	139.6(7)
Tb1–O5b	277.0(4)		ø = 246.0		ø = 137.7
	ø = 250.0				
Ho1–O3a	232.8(3)	Ho2–O2a	224.8(3)	B1–O6	141.8(5)
Ho1–O4	232.9(3)	Ho2–O2b	229.2(3)	B1–O2	145.6(6)
Ho1–O6a	234.3(3)	Ho2–O6	235.3(3)	B1–O4	149.9(5)
Ho1–O5a	235.4(3)	Ho2–O5	238.9(3)	B1–O1	157.1(6)
Ho1–F1	242.1(3)	Ho2–O1	239.9(3)		ø = 148.6
Ho1–O3b	244.2(3)	Ho2–O3	242.2(3)		
Ho1–O1	254.6(3)	Ho2–F1a	244.6(3)	B2–O5	136.8(6)
Ho1–O2	262.6(3)	Ho2–F1b	256.5(3)	B2–O3	137.6(5)
Ho1–O6b	265.2(3)	Ho2–F1c	281.9(4)	B2–O1	139.6(6)
Ho1–O5b	276.8(3)		ø = 243.7		ø = 138.0
	ø = 248.1				
Er1–O3a	231.0(3)	Er2–O2a	224.0(3)	B1–O6	142.0(5)
Er1–O4	231.6(3)	Er2–O2b	227.7(3)	B1–O2	145.2(7)
Er1–O5a	233.1(3)	Er2–O6	233.6(3)	B1–O4	149.2(6)
Er1–O6a	233.8(4)	Er2–O5	237.7(4)	B1–O1	157.7(7)
Er1–F1	240.9(4)	Er2–O1	238.6(3)		ø = 148.5
Er1–O3b	242.9(3)	Er2–O3	242.4(4)		
Er1–O1	253.7(3)	Er2–F1a	242.9(3)	B2–O5	136.2(7)
Er1–O2	262.0(3)	Er2–F1b	258.0(3)	B2–O3	138.9(6)
Er1–O6b	263.7(4)	Er2–F1c	280.4(4)	B2–O1	140.5(7)
Er1–O5b	276.8(4)		ø = 242.8		ø = 138.5
	ø = 247.0				

Sm^{3+} (127.2 pm), Eu^{3+} (126.0 pm), Gd^{3+} (124.7 pm), Tb^{3+} (123.5 pm), Dy^{3+} (122.3 pm), Ho^{3+} (121.2 pm), and Er^{3+} (120.2 pm). Since the differences in size are not too large, the bond lengths and angles of $RE_4B_4O_{11}F_2$ (RE = Sm, Tb, Ho, Er) are comparable to the values found in the other isotypic compounds [12, 13]. As expected, the RE–O/F distances in $RE_4B_4O_{11}F_2$ (RE = Pr, Nd, Sm–Er) decrease slightly but still significantly from values within 237.9(3)–285.5(3) pm in $Pr_4B_4O_{11}F_2$ and 231.0(3)–276.8(4) pm in $Er_4B_4O_{11}F_2$. The crystal structure of $RE_4B_4O_{11}F_2$ (RE = Pr, Nd, Sm–Er) contains a distorted tetrahedron that was interpreted as a BO_3 group, in which the boron atom is drawn towards a fourth oxygen atom, resulting in a long B–O bond [12]. This long B1–O1 bond hardly varies in all nine isotypic compounds. The shortest B1–O1 bond measures 156.6(8) pm in $Dy_4B_4O_{11}F_2$ [13], the longest B1–O1 bond with a value of 159.0(6) pm is found in $Gd_4B_4O_{11}F_2$ [12]. The B1–O1 bond lengths in $RE_4B_4O_{11}F_2$ (RE = Sm, Tb, Ho, Er) all lie within these values. Obviously, the changing ionic radii of the rare earth cations have no influence on the B1–O1 bond length. The BO_3 groups in $RE_4B_4O_{11}F_2$ (RE = Sm, Tb, Ho, Er) have average B–O distances between 137.7 and 138.5 pm – in good agreement with the literature value of 137.0 pm [26].

The bond valence sums of all atoms in $RE_4B_4O_{11}F_2$ (RE = Sm, Tb, Ho, Er) were calculated according to the BLBS (bond length/bond strength, ΣV) [27–31] and the CHARDI (charge distribution in solids, ΣQ) concept [29, 30, 32]. The results of both calculations verify the formal valence states in the fluoride borates. Table 6 shows the formal ionic charges received from the calculations, which fit well to the expected values.

Furthermore, we calculated the MAPLE values (Madelung Part of Lattice Energy) [33–35] of $RE_4B_4O_{11}F_2$ (RE = Sm, Tb, Ho, Er) and compared them with the values for the binary components. We obtained a value of 72 178 kJ mol^{-1} for $Sm_4B_4O_{11}F_2$, to be compared with 72 227 kJ mol^{-1} (deviation: 0.07%) starting from the binary components [5/3 × Sm_2O_3 ([36], 14 767 kJ mol^{-1}) + 2 × B_2O_3-II ([37], 21 938 kJ mol^{-1}) +2/3 × SmF_3 ([38], 5608 kJ mol^{-1})]. For $Tb_4B_4O_{11}F_2$, the resulting value is 72 667 kJ mol^{-1} compared to 72 723 kJ mol^{-1} (deviation: 0.08%) based on the binary components [5/3 × Tb_2O_3 ([39], 15 053 kJ mol^{-1}) +2 × B_2O_3-II ([37], 21 938 kJ mol^{-1}) +2/3 × TbF_3 ([40], 5636 kJ mol^{-1})]. For $Ho_4B_4O_{11}F_2$, we obtained a value of 72 824 kJ mol^{-1}, to be compared with 72 901 kJ mol^{-1} (deviation: 0.11%) starting from the binary components [5/3 × Ho_2O_3 ([41], 15 134 kJ mol^{-1}) +2 × B_2O_3-II ([37], 21 938 kJ mol^{-1}) +2/3 × HoF_3 ([42], 5703 kJ mol^{-1})]. For $Er_4B_4O_{11}F_2$, the resulting value is 72 912 kJ mol^{-1} compared to 73 199 kJ mol^{-1} (deviation: 0.39%) based on the binary components [5/3 × Er_2O_3 ([43], 15 283 kJ mol^{-1}) +2 × B_2O_3-II ([37], 21 938 kJ mol^{-1}) +2/3 × ErF_3 ([44], 5777 kJ mol^{-1})].

4 Conclusion

With the syntheses of $RE_4B_4O_{11}F_2$ (RE = Sm, Tb, Ho, Er), the possible formation range of compounds with the composition $RE_4B_4O_{11}F_2$ has been extensively investigated and

Table 4: Interatomic angles (deg) in $RE_4B_4O_{11}F_2$ (RE = Sm, Tb, Ho, Er) (space group: $C2/c$), calculated with the single-crystal lattice parameters (standard deviations in parentheses).

O6–B1–O2	115.7(3)	O5–B2–O3	118.4(3)	Sm1–F1–Sm2a	100.0(1)
O6–B1–O4	114.7(3)	O5–B2–O1	122.3(3)	Sm1–F1–Sm2b	99.1(1)
O2–B1–O4	106.9(3)	O3–B2–O1	119.2(3)	Sm1–F1–Sm2c	103.9(1)
O6–B1–O1	115.2(3)		ø = 120.0	Sm2a–F1–Sm2b	133.0(2)
O2–B1–O1	103.6(3)			Sm2a–F1–Sm2c	112.2(1)
O4–B1–O1	99.0(3)			Sm2b–F1–Sm2c	104.1(1)
	ø = 109.2				ø = 108.7
O6–B1–O2	115.5(5)	O5–B2–O3	119.1(5)	Tb1–F1–Tb2a	100.8(2)
O6–B1–O4	115.0(5)	O5–B2–O1	121.8(5)	Tb1–F1–Tb2b	98.7(2)
O2–B1–O4	107.2(4)	O3–B2–O1	119.0(5)	Tb1–F1–Tb2c	103.2(2)
O6–B1–O1	114.9(5)		ø = 120.0	Tb2a–F1–Tb2b	133.2(2)
O2–B1–O1	103.6(4)			Tb2a–F1–Tb2c	112.3(2)
O4–B1–O1	98.7(4)			Tb2b–F1–Tb2c	103.8(2)
	ø = 109.2				ø = 108.7
O6–B1–O2	116.1(4)	O5–B2–O3	118.5(4)	Ho1–F1–Ho2a	101.3(2)
O6–B1–O4	114.5(4)	O5–B2–O1	122.4(4)	Ho1–F1–Ho2b	98.3(2)
O2–B1–O4	107.1(3)	O3–B2–O1	119.0(4)	Ho1–F1–Ho2c	102.6(2)
O6–B1–O1	115.2(4)		ø = 120.0	Ho2a–F1–Ho2b	133.2(2)
O2–B1–O1	103.5(3)			Ho2a–F1–Ho2c	112.5(2)
O4–B1–O1	98.5(3)			Ho2b–F1–Ho2c	103.9(1)
	ø = 109.2				ø = 108.6
O6–B1–O2	116.4(4)	O5–B2–O3	118.9(5)	Er1–F1–Er2a	101.5(2)
O6–B1–O4	114.7(4)	O5–B2–O1	122.5(4)	Er1–F1–Er2b	97.9(2)
O2–B1–O4	107.4(4)	O3–B2–O1	118.5(5)	Er1–F1–Er2c	102.9(2)
O6–B1–O1	114.6(4)		ø = 120.0	Er2a–F1–Er2b	132.7(2)
O2–B1–O1	103.1(4)			Er2a–F1–Er2c	112.8(2)
O4–B1–O1	98.5(3)			Er2b–F1–Er2c	104.1(2)
	ø = 109.1				ø = 108.6

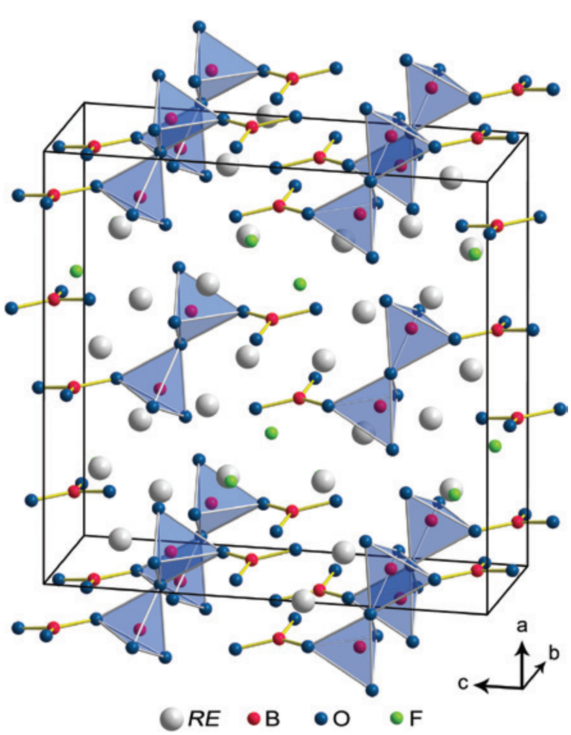

Fig. 2: Crystal structure of $RE_4B_4O_{11}F_2$ (RE = Sm, Tb, Ho, Er) showing the fundamental building block 2Δ2□:Δ□□Δ.

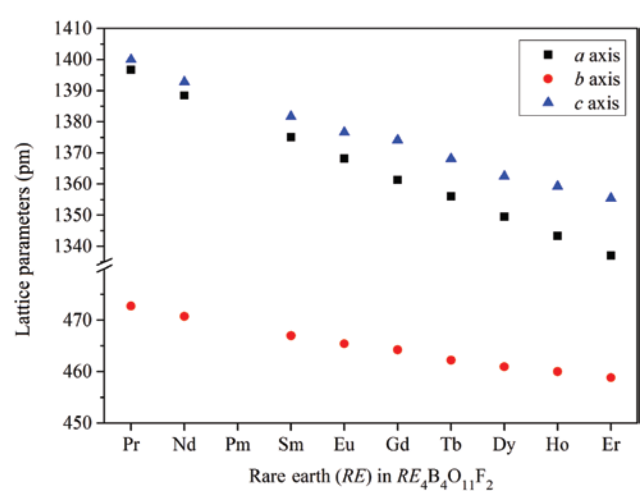

Fig. 3: Visualization of the progression of the lattice parameters (in pm) of $RE_4B_4O_{11}F_2$ (RE = Pr, Nd, Sm–Er) with the typical decrease due to the lanthanoid contraction.

the number of isotypic compounds with the constitution $RE_4B_4O_{11}F_2$ has been extended to nine. The existence of the compound "$Ce_4B_4O_{11}F_2$" could still not be proven but would be of great interest as it is the missing link between the different crystal structures of $La_4B_4O_{11}F_2$ and $Pr_4B_4O_{11}F_2$.

Table 5: Comparison of the single-crystal lattice parameters (pm, deg) and unit cell volumes (nm^3) of $RE_4B_4O_{11}F_2$ (RE = Pr, Nd, Sm–Er) (standard deviations in parentheses).

Compound	*a*	*b*	*c*	*β*	*V*
$Pr_4B_4O_{11}F_2$	1396.7(5)	472.7(2)	1400.0(3)	91.1(1)	0.9242(3)
$Nd_4B_4O_{11}F_2$	1388.4(4)	470.7(2)	1392.8(5)	91.1(1)	0.9100(3)
$Sm_4B_4O_{11}F_2$	1375.06(1)	466.95(2)	1381.66(4)	91.1(1)	0.88698(5)
$Eu_4B_4O_{11}F_2$	1368.2(3)	465.4(1)	1376.6(3)	91.2(1)	0.8765(3)
$Gd_4B_4O_{11}F_2$	1361.3(3)	464.2(2)	1374.1(3)	91.3(1)	0.8681(3)
$Tb_4B_4O_{11}F_2$	1356.0(3)	462.20(9)	1368.1(3)	91.2(1)	0.8573(3)
$Dy_4B_4O_{11}F_2$	1349.5(3)	460.9(1)	1362.5(3)	91.3(1)	0.8472(3)
$Ho_4B_4O_{11}F_2$	1343.3(3)	459.99(9)	1359.2(3)	91.4(1)	0.8396(3)
$Er_4B_4O_{11}F_2$	1337.0(3)	458.82(9)	1355.4(3)	91.4(1)	0.8312(3)

Table 6: Charge distribution in $RE_4B_4O_{11}F_2$ (RE = Sm, Tb, Ho, Er), calculated according to the BLBS (ΣV) [27–31] and the CHARDI concept (ΣQ) [29, 30, 32].

	Sm1	**Sm2**	**B1**	**B2**	**Tb1**	**Tb2**	**B1**	**B2**
ΣV	3.14	3.02	2.94	2.94	3.08	2.99	2.99	2.96
ΣQ	2.98	3.03	2.98	3.01	2.97	3.05	2.97	3.01
	O1	**O2**	**O3**	**O4**	**O1**	**O2**	**O3**	**O4**
ΣV	−2.10	−2.03	−2.15	−2.27	−2.11	−2.02	−2.14	−2.31
ΣQ	−1.98	−1.99	−2.12	−2.20	−1.97	−1.98	−2.14	−2.26
	O5	**O6**	**F1**		**O5**	**O6**	**F1**	
ΣV	−1.91	−1.91	−0.80		−1.91	−1.91	−0.77	
ΣQ	−1.89	−1.93	−0.99		−1.88	−1.93	−0.96	
	Ho1	**Ho2**	**B1**	**B2**	**Er1**	**Er2**	**B1**	**B2**
ΣV	3.03	3.00	2.97	2.93	3.04	2.99	2.97	2.89
ΣQ	3.04	3.09	2.90	2.97	2.99	3.07	2.94	3.00
	O1	**O2**	**O3**	**O4**	**O1**	**O2**	**O3**	**O4**
ΣV	−2.12	−2.02	−2.09	−2.29	−2.09	−2.02	−2.05	−2.32
ΣQ	−2.25	−1.99	−2.12	−2.25	−1.98	−2.00	−2.06	−2.29
	O5	**O6**	**F1**		**O5**	**O6**	**F1**	
ΣV	−1.92	−1.89	−0.74		−1.94	−1.89	−0.75	
ΣQ	−1.65	−1.94	−0.92		−1.97	−1.94	−0.91	

Acknowledgement: We thank Dr. G. Heymann (Leopold-Franzens-Universität Innsbruck, Austria) for collecting the single-crystal data. The research was funded by the Austrian Science Fund (FWF): P 23212-N19.

References

[1] G. Su, H. Toratani, *Jpn. Kokai Tokkyo Koho* **1997**, 6.
[2] T. Suzuki, M. Hirano, H. Hosono, *J. Appl. Phys.* **2002**, *91*, 4149.
[3] L. R. P. Kassab, L. C. Courrol, A. S. Morais, S. H. Tatumi, N. U. Wetter. L. Gomes, *J. Opt. Soc. Am. B: Opt. Phys.* **2002**, *19*, 2921.
[4] C. K. Jayasankar, V. Venkatramu, P. Babu, Th. Troster, W. Sievers, G. Wortmann, W. B. Holzapfel, *J. Appl. Phys.* **2005**, *97*, 093523-1.
[5] W. A. Pisarski, J. Pisarska, M. Mączka, W. Ryba-Romanowski, *J. Mol. Struct.* **2006**, *792–293*, 207.
[6] A. V. Ravi Kumar, B. Apparao, N. Veeraiah, *Bull. Mater. Sci.* **1998**, *21*, 341.
[7] H. A. Höppe, *Z. Naturforsch.* **2015**, *70b*, 769.
[8] H. Huppertz, *Chem. Commun.* **2011**, *47*, 131.
[9] A. Pitscheider, *PhD thesis*, Universität Innsbruck, Innsbruck, **2011**.
[10] A. Haberer, R. Kaindl, O. Oeckler, H. Huppertz, *J. Solid State Chem.* **2010**, *183*, 1970.
[11] P. C. Burns, J. D. Grice, F. C. Hawthorne, *Can. Mineral.* **1995**, *33*, 1131.
[12] A. Haberer, R. Kaindl, H. Huppertz, *J. Solid State Chem.* **2010**, *183*, 471.
[13] A. Pitscheider, M. Enders, H. Huppertz, *Z. Naturforsch.* **2010**, *65b*, 1439.
[14] M. Glätzle, H. Huppertz, *Z. Naturforsch.* **2013**, *68b*, 635.
[15] D. Walker, M. A. Carpenter, C. M. Hitch, *Am. Mineral.* **1990**, *75*, 1020.
[16] D. Walker, *Am. Mineral.* **1991**, *76*, 1092.
[17] H. Huppertz, *Z. Kristallogr.* **2004**, *219*, 330.
[18] D. C. Rubie, *Phase Transitions* **1999**, *68*, 431.
[19] N. Kawai, S. Endo, *Rev. Sci. Instrum.* **1970**, *8*, 1178.
[20] H. Emme, H. Huppertz, *Acta Crystallogr.* **2005**, *C61*, 29.
[21] H. Emme, M. Valldor, R. Pöttgen, H. Huppertz, *Chem. Mater.* **2005**, *17*, 2707.
[22] Z. SCALEPACK, W. Otwinowski, Minor in *Methods in Enzymology*, Vol. 276, *Macromolecular Crystallography*, Part A (Eds.: C. W. Carter Jr., R. M. Sweet), Academic Press, New York, **1997**, p. 307.
[23] G. M. Sheldrick, SHELXS/L-97, *Programm Suite for the Solution and Refinement of Crystal Structures*, University of Göttingen, Göttingen (Germany) **1997**.
[24] G. M. Sheldrick, *Acta Crystallogr.* **2008**, *A64*, 112.
[25] R. D. Shannon, *Acta Crystallogr.* **1976**, *A32*, 751.
[26] E. Zobetz, *Z. Kristallogr.* **1982**, *160*, 81.
[27] L. Pauling, *J. Am. Chem. Soc.* **1947**, *69*, 542.
[28] A. Byström, K.-A. Wilhelmi, *Acta Chem. Scand.* **1951**, *5*, 1003.
[29] I. D. Brown, D. Altermatt, *Acta Crystallogr.* **1985**, *B41*, 244.
[30] N. E. Brese, M. O'Keeffe, *Acta Crystallogr.* **1991**, *B47*, 192.
[31] N. E. Brese, M. O'Keeffe, *Structure and Bonding*, Springer-Verlag, Berlin, **1989**.
[32] R. Hoppe, S. Voigt, H. Glaum, J. Kissel, H. P. Müller, K. J. Bernet, *J. Less-Common Met.* **1989**, *156*, 105.
[33] R. Hoppe, *Angew. Chem., Int. Ed. Engl.* **1966**, *5*, 96.

[34] R. Hoppe, *Angew. Chem., Int. Ed. Engl.* **1970**, *9*, 25.
[35] R. Hübenthal, M. Serafin, R. Hoppe, Maple (version 4.0), *Program for the Calculation of Distances, Angles, Effective Coordination Numbers, Coordination Spheres, and Lattice Energies*, University of Gießen, Gießen (Germany) **1993**.
[36] Y. Tabira, R. L. Withers, *J. Solid State Chem*. **1999**, *148*, 205.
[37] C. T. Prewitt, R. D. Shannon, *Acta Crystallogr.* **1968**, *B24*, 869.
[38] G.-Q. Wu, R. Hoppe, *Z. Anorg. Allg. Chem*. **1984**, *514*, 99.
[39] E. Hubbert-Paletta, Hk. Müller-Buschbaum, *Z. Anorg. Allg. Chem*. **1968**, *363*, 145.
[40] M. Piotrowski, A. Murasik, *Phys. Stat. Sol.* **1985**, *A89*, 571.
[41] S. A. Hering, H. Huppertz, *Z. Naturforsch*. **2009**, *64b*, 1032.
[42] M. Piotrowski, H. Ptasiewicz-bak, A. Murasik, *Phys. Stat. Sol*. **1979**, *A55*, K163.
[43] H. R. Hoekstra, *Inorg. Chem*. **1966**, *5*, 754.
[44] A. Zalkin, D. H. Templeton, *J. Am. Chem. Soc.* **1953**, *75*, 2453.